AIAA JOURNAL
Vol. 36, No. 9, September 1998

Influence of Curing Stresses on Extension–Twist Coupling in Laminated Composite Strips

Andrew Makeev,* Erian A. Armanios,† and David Hooke‡
Georgia Institute of Technology, Atlanta, Georgia 30332-0150

An analytical model developed previously for the finite displacement of laminated composite strips exhibiting extension–twist coupling is extended to include the influence of hygrothermal stresses. A closed-form expression for the twist associated with the curing stresses is derived. The relationship between applied extension and twist is obtained in closed form as well, and the contribution of the curing stresses is isolated. A set of angle-ply laminated composite strips made of a graphite/cyanate material system is manufactured and tested. A custom-made air bearing apparatus is used in the testing to allow one end of the strip to twist as axial load is applied. Test results depict the nonlinear axial force–twist behavior, and the analytical predictions are in close agreement with test data and a geometrically nonlinear finite element simulation.

Introduction

COUPLING of deformation modes in laminated composites is a unique tailoring tool that provides additional flexibility to meet design requirements efficiently and economically. An example is extension–twist coupling, which could be implemented in composite rotor blades to control twisting motions at different rotor speeds. Such a coupling is achieved in laminated composites by using antisymmetric angle-ply stacking sequences. These layups lead to hygrothermal warping due to the curing stresses and result in a finite twist of the laminate. Moreover, the relatively small torsional-to-extensional-stiffness ratio in these laminates leads to finite twisting rotation as axial load is applied. These geometrically nonlinear effects fall beyond the small displacement assumption of classical lamination theory and need to be accounted for. To this end, a geometrically nonlinear shell-type analysis was developed in Ref. 1. The analysis was based on the assumption that a straight line element perpendicular to the middle surface before deformation remains straight and inextensible. Closed-form axial force–twist relationships were obtained, and a number of approximate models were derived. It was found that the variation of average transverse normal strain along the width and the free-edge boundary conditions have an insignificant influence on the axial force–twist behavior. The twisting moment due to the axial stress resultants was found to represent the major contribution to the nonlinear behavior. This analytical model is extended in the present work to account for the influence of hygrothermal stresses. Manufacturing and testing programs are developed to validate the analytical predictions by comparison with test data. Comparison of analytical predictions with a geometrically nonlinear finite element simulation is also performed.

The analytical model is presented first, leading to a closed-form expression for the induced twist associated with the curing stresses. A closed-form expression is also derived for the axial force–twist relationship. This is followed by a description of the manufacturing and testing programs. Finally, a comparison is presented among the analytical predictions, finite element simulation, and test data.

Development of Analytical Model

Displacement Field

The fundamental concept in developing a simple model for the extension–finite twist behavior of a beam lies in isolating the contributions of the small and finite displacement fields. The form of the finite displacements is derived by considering the rotation of a thin-walled beam cross section. The associated out-of-plane strains are brought to zero by rotating the straight line elements perpendicular to the middle surface in the undeformed state. The resulting finite displacement field is subsequently modified by a small displacement field to account for all elastic strain components and to satisfy the boundary conditions.

Consider the laminated composite strip shown in Fig. 1. Its thickness h is small relative to the width $2b$, and its length L is large compared to the width. The laminate has a constant initial twist rate θ_0 and is undergoing a constant elastic twist rate q about the x axis. The associated strains are considered small and independent of x, and the material is assumed to be linearly elastic. The position vector of a material point in the initial state is derived kinematically by considering a finite twist of the initially flat strip, assuming no out-of-plane strains, and keeping terms up to $O(\theta_0 y)^2$. The result is expressed as

$$\boldsymbol{r}_0 = (x - \theta_0 yz)\hat{\boldsymbol{i}} + y\hat{\boldsymbol{e}}_{20} + z\left[1 - \tfrac{1}{2}(\theta_0 y)^2\right]\hat{\boldsymbol{e}}_{30} \tag{1}$$

where the $\hat{\boldsymbol{e}}_{20}$ and $\hat{\boldsymbol{e}}_{30}$ are the unit vectors in the plane of the cross section in the initial state following the transformation:

$$\hat{\boldsymbol{e}}_{20} = \cos(\theta_0 x)\hat{\boldsymbol{j}} + \sin(\theta_0 x)\hat{\boldsymbol{k}}, \qquad \hat{\boldsymbol{e}}_{30} = -\sin(\theta_0 x)\hat{\boldsymbol{j}} + \cos(\theta_0 x)\hat{\boldsymbol{k}} \tag{2}$$

The unit base vectors associated with the reference Cartesian coordinate system x, y, and z, appearing in Fig. 1, are denoted by $\hat{\boldsymbol{i}}$, $\hat{\boldsymbol{j}}$, and $\hat{\boldsymbol{k}}$, respectively.

The position vector of the material point in the deformed state is

$$\boldsymbol{r} = [x - (\theta + \theta_0)yz + u]\hat{\boldsymbol{i}} + (y + v)\hat{\boldsymbol{e}}_2 + \left\{z\left[1 - \tfrac{1}{2}(\theta + \theta_0)^2 y^2\right] + w\right\}\hat{\boldsymbol{e}}_3 \tag{3}$$

where $\hat{\boldsymbol{e}}_2$ and $\hat{\boldsymbol{e}}_3$ are the unit vectors expressed as

$$\hat{\boldsymbol{e}}_2 = \cos(\theta_0 + \theta)x\hat{\boldsymbol{j}} + \sin(\theta_0 + \theta)x\hat{\boldsymbol{k}}$$
$$\hat{\boldsymbol{e}}_3 = -\sin(\theta_0 + \theta)x\hat{\boldsymbol{j}} + \cos(\theta_0 + \theta)x\hat{\boldsymbol{k}} \tag{4}$$

and

$$u = \varepsilon_0 x + U(y, z), \qquad v = V(y, z), \qquad w = W(y, z) \tag{5}$$

are the components of the small displacement vector

$$\boldsymbol{u} = u\hat{\boldsymbol{i}} + v\hat{\boldsymbol{e}}_2 + w\hat{\boldsymbol{e}}_3 \tag{6}$$

which accounts for all deformation modes. The axial strain is denoted by ε_0 in Eq. (5).

Received Sept. 26, 1997; revision received May 8, 1998; accepted for publication May 15, 1998.

*Graduate Research Assistant, School of Aerospace Engineering; currently Postdoctoral Fellow, School of Aerospace Engineering.
†Professor, School of Aerospace Engineering. Associate Fellow AIAA.
‡Graduate Research Assistant, School of Aerospace Engineering; currently Engineer, Lockheed Martin Skunk Works, 1011 Lockheed Way, Palmdale, CA 93599-2543.

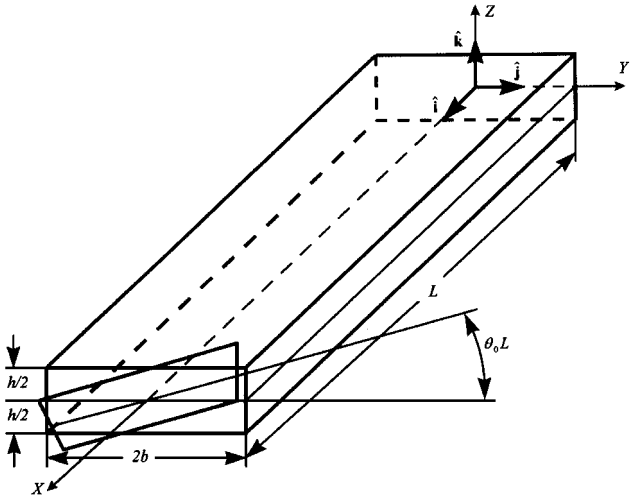

Fig. 1 Laminated strip geometry and coordinate system.

Consistent with the thin-walled strip geometry, the following bounds are imposed on the geometric and displacement variables:

$$\left(\frac{h}{b}\right)^2 = O(\varepsilon), \qquad (\theta b)^2, (\theta_0 b)^2 = O(\varepsilon)$$

$$\frac{\partial U}{\partial y}, \frac{\partial U}{\partial z}, \frac{\partial V}{\partial y}, \frac{\partial V}{\partial z}, \frac{\partial W}{\partial y}, \frac{\partial W}{\partial z} = O(\varepsilon) \tag{7}$$

$$(\theta V), (\theta W), (\theta_0 V), (\theta_0 W) = O\left(\varepsilon^{\frac{3}{2}}\right)$$

where ε denotes the magnitude of the maximum strain. Terms up to $O(\varepsilon)$ will be kept in the strain-displacement relationships. A development keeping terms of higher order shows a negligible influence on the axial force–twist relationship.[2]

The Lagrangian strain tensor components are defined as[3]

$$2\varepsilon_{ij} = g_{ij} - h_{ij} \tag{8}$$

where g_{ij} and h_{ij} are the metric tensor components associated with the final and initial states, respectively,

$$g_{ij} = \frac{\partial \boldsymbol{r}}{\partial x^i} \cdot \frac{\partial \boldsymbol{r}}{\partial x^j}, \qquad h_{ij} = \frac{\partial \boldsymbol{r}_0}{\partial x^i} \cdot \frac{\partial \boldsymbol{r}_0}{\partial x^j} = \delta_{ij}$$
$$(x^1 = x,\ x^2 = y, x^3 = z) \tag{9}$$

Substitute Eqs. (1) and (3) into Eqs. (8) and (9) to get, for the engineering strain components,

$$\varepsilon_{xx} = \varepsilon_0 + \frac{1}{2}\left(\theta^2 + 2\theta\theta_0\right)y^2, \qquad \varepsilon_{yy} = \frac{\partial V}{\partial y}, \qquad \varepsilon_{zz} = \frac{\partial W}{\partial z} \tag{10}$$

$$\gamma_{xz} = \frac{\partial U}{\partial z}, \qquad \gamma_{yz} = \frac{\partial V}{\partial z} + \frac{\partial W}{\partial y}, \qquad \gamma_{xy} = \frac{\partial U}{\partial y} - 2\theta z$$

Because the strip is thin, the transverse shear strain components in Eq. (10) will be approximated by their average through-the-thickness values

$$\gamma_{yz} = \gamma_{yz}(y), \qquad \gamma_{xz} = \gamma_{xz}(y) \tag{11}$$

Moreover, the normals are assumed to be inextensible, that is,

$$\varepsilon_{zz} = 0 \tag{12}$$

Allowing for nonzero transverse normal strain is shown in Ref. 1 to have a negligible influence on the axial force–twist predictions.

Integrate the third, fourth, and fifth equations in Eq. (10) and use the approximation in Eqs. (11) and (12) to get

$$U = U_0(y) - zU_1(y), \qquad V = V_0(y) - zV_1(y), \qquad W = W_0(y) \tag{13}$$

Substituting Eq. (13) into Eq. (10), the strain components can be expressed as

$$\varepsilon_{xx} = \varepsilon^0_{xx} = \varepsilon_0 + \frac{1}{2}\left(\theta^2 + 2\theta\theta_0\right)y^2$$

$$\varepsilon_{yy} = \varepsilon^0_{yy} - z\kappa_{yy} = \frac{\partial V_0}{\partial y} - z\frac{\partial V_1}{\partial y}, \qquad \varepsilon_{zz} = 0$$

$$\gamma_{yz} = \gamma^0_{yz} = \frac{\partial W_0}{\partial y} - V_1, \qquad \gamma_{xz} = \gamma^0_{xz} = -U_1 \tag{14}$$

$$\gamma_{xy} = \gamma^0_{xy} - z\kappa_{xy} = \frac{\partial U_0}{\partial y} - z\left(\frac{\partial U_1}{\partial y} + 2\theta\right)$$

Superscript 0 associated with the strain components in Eq. (14) denote middle surface values.

Equilibrium Equations

The equilibrium equations and associated boundary conditions are derived from the principle of virtual work. For a cantilevered strip subjected to an axial force F and a torque M, the principle of virtual work is written as

$$\delta U - M\delta\theta - F\delta\varepsilon_0 = 0 \tag{15}$$

The variation of the strain energy per unit length is expressed as

$$\delta U = \int_{-b}^{b} \mathrm{d}y \int_{-h/2}^{h/2} \sigma^{ij}\delta\varepsilon_{ij}\sqrt{g}\,\mathrm{d}z \qquad (i, j = x, y, z) \tag{16}$$

where σ^{ij} are the second Piola–Kirchhoff stress tensor components. Summation over the repeated indices is assumed. The Jacobian $\sqrt{g}$ can be represented as

$$\sqrt{g} = \frac{\partial \boldsymbol{r}_0}{\partial x} \cdot \left(\frac{\partial \boldsymbol{r}_0}{\partial y} \times \frac{\partial \boldsymbol{r}_0}{\partial z}\right) = 1 \tag{17}$$

if terms of $O(\varepsilon)$ are neglected compared to 1.

The forces and moments per unit middle surface length are defined as

$$(N_{xx}, N_{yy}, Q_y, Q_x, N_{xy}, M_{xx}, M_{yy}, M_{xy})$$
$$= \int_{-h/2}^{h/2} (\sigma_{xx}, \sigma_{yy}, \sigma_{yz}, \sigma_{xz}, \sigma_{xy}, z\sigma_{xx}, z\sigma_{yy}, z\sigma_{xy})\,\mathrm{d}z \tag{18}$$

where the subscripts do not denote covariant tensor components.

Substitute from Eqs. (14), (16), and (17) into Eq. (15) and use Eq. (18) to get

$$N_{yy} = Q_y = N_{xy} = M_{yy} = 0 \tag{19}$$

$$M_{xy}|_{y=\pm b} = 0 \tag{20}$$

$$\frac{\partial M_{xy}}{\partial y} - Q_x = 0 \tag{21}$$

$$\int_{-b}^{b} N_{xx}\,\mathrm{d}y = F \tag{22}$$

$$\int_{-b}^{b} \left[N_{xx}y^2(\theta + \theta_0) - 2M_{xy}\right]\mathrm{d}y = M \tag{23}$$

The term $N_{xx}y^2(\theta + \theta_0)$ in Eq. (23) represents the contribution of the axial forces to the twisting moment. This term was shown in Ref. 1 to have a major contribution to the nonlinear behavior in the axial-force twist relationship.

Constitutive Relationships

The constitutive relationships for the laminated composite strip are expressed as

$$\begin{Bmatrix} N_{xx} \\ N_{yy} \\ N_{xy} \\ M_{xx} \\ M_{yy} \\ M_{xy} \end{Bmatrix} = \begin{bmatrix} A_{11} & A_{12} & A_{16} & B_{11} & B_{12} & B_{16} \\ A_{12} & A_{22} & A_{26} & B_{12} & B_{22} & B_{26} \\ A_{16} & A_{26} & A_{66} & B_{16} & B_{26} & B_{66} \\ B_{11} & B_{12} & B_{16} & D_{11} & D_{12} & D_{16} \\ B_{12} & B_{22} & B_{26} & D_{12} & D_{22} & D_{26} \\ B_{16} & B_{26} & B_{66} & D_{16} & D_{26} & D_{66} \end{bmatrix} \begin{Bmatrix} \varepsilon^0_{xx} \\ \varepsilon^0_{yy} \\ \gamma^0_{xy} \\ -\kappa_{xx} \\ -\kappa_{yy} \\ -\kappa_{xy} \end{Bmatrix} - \begin{Bmatrix} N_{xx} \\ N_{yy} \\ N_{xy} \\ M_{xx} \\ M_{yy} \\ M_{xy} \end{Bmatrix}^{\mathrm{HT}} \tag{24}$$

$$\begin{Bmatrix} Q_y \\ Q_x \end{Bmatrix} = \begin{bmatrix} A_{44} & A_{45} \\ A_{45} & A_{55} \end{bmatrix} \begin{Bmatrix} \gamma_{yz} \\ \gamma_{xz} \end{Bmatrix} \tag{25}$$

Equations (24) and (25) are similar to the constitutive relationships of classical lamination theory. The strains and curvatures account for finite twist as defined in Eq. (14). The in-plane A_{ij}, coupling B_{ij}, and bending D_{ij} stiffness coefficients are defined as

$$(A_{ij}, B_{ij}, D_{ij}) = \int_{-h/2}^{h/2} \bar{Q}_{ij}(1, z, z^2)\,\mathrm{d}z \tag{26}$$

where $\bar{Q}_{ij}$ are the laminate plane stress reduced stiffness coefficients in the x, y, z coordinate system.[4] Note that Eq. (12) implies for each lamina that

$$E_{33} \to \infty, \qquad \nu_{13} = \nu_{23} = 0 \tag{27}$$

where indices 1, 2, and 3 are the principal material axes and E_{33}, ν_{13}, and ν_{23} are Young's modulus and Poisson's ratios associated with the transverse normal direction. Therefore, the in-plane stiffness coefficients $\bar{Q}_{ij}$ can be calculated using the plane stress assumption.[4]

The hygrothermal forces and moments per unit middle surface length, denoted with superscript HT in Eq. (24), are defined as

$$\left(\begin{Bmatrix} N_{xx} \\ N_{yy} \\ N_{xy} \end{Bmatrix}^{\mathrm{HT}}, \begin{Bmatrix} M_{xx} \\ M_{yy} \\ M_{xy} \end{Bmatrix}^{\mathrm{HT}} \right) = \int_{-h/2}^{h/2} \begin{bmatrix} \bar{Q}_{11} & \bar{Q}_{12} & \bar{Q}_{16} \\ \bar{Q}_{12} & \bar{Q}_{22} & \bar{Q}_{26} \\ \bar{Q}_{16} & \bar{Q}_{26} & \bar{Q}_{66} \end{bmatrix} \times \begin{bmatrix} \alpha_{xx} & \beta_{xx} \\ \alpha_{yy} & \beta_{yy} \\ \alpha_{xy} & \beta_{xy} \end{bmatrix} \begin{Bmatrix} \Delta T \\ \Delta H \end{Bmatrix} (1, z)\,\mathrm{d}z \tag{28}$$

The linear coefficients of thermal expansion and moisture swelling are denoted by α_{ij} and β_{ij}, respectively. The change in temperature is denoted by ΔT and in moisture weight gain percentage by ΔH.

For antisymmetric stacking sequences producing extension–twist coupling, the following stiffness coefficients in Eq. (24) vanish:

$$A_{16} = A_{26} = A_{45} = D_{16} = D_{26} = B_{11} = B_{22} = B_{12} = B_{66} = 0 \tag{29}$$

As a result the constitutive relationships take the following decoupled form:

$$\begin{Bmatrix} N_{xx} \\ N_{yy} \\ M_{xy} \end{Bmatrix} = \begin{bmatrix} A_{11} & A_{12} & B_{16} \\ A_{12} & A_{22} & B_{26} \\ B_{16} & B_{26} & D_{66} \end{bmatrix} \begin{Bmatrix} \varepsilon^0_{xx} \\ \varepsilon^0_{yy} \\ -\kappa_{xy} \end{Bmatrix} - \begin{Bmatrix} N_{xx} \\ N_{yy} \\ M_{xy} \end{Bmatrix}^{\mathrm{HT}} \tag{30}$$

$$\begin{Bmatrix} N_{xy} \\ M_{xx} \\ M_{yy} \end{Bmatrix} = \begin{bmatrix} A_{66} & B_{16} & B_{26} \\ B_{16} & D_{11} & D_{12} \\ B_{26} & D_{12} & D_{66} \end{bmatrix} \begin{Bmatrix} \gamma^0_{xy} \\ -\kappa_{xx} \\ -\kappa_{yy} \end{Bmatrix} - \begin{Bmatrix} N_{xy} \\ M_{xx} \\ M_{yy} \end{Bmatrix}^{\mathrm{HT}}$$

$$Q_y = A_{44}\gamma_{yz}, \qquad Q_x = A_{55}\gamma_{xz} \tag{31}$$

Substituting from Eqs. (19) and (14), Eqs. (30) and (31) reduce to

$$\begin{Bmatrix} N_{xx} \\ M_{xy} \end{Bmatrix} = \begin{bmatrix} \psi_{11} & \psi_{12} \\ \psi_{12} & \psi_{22} \end{bmatrix} \begin{Bmatrix} \varepsilon_0 + \frac{1}{2}\left(\theta^2 + 2\theta\theta_0\right)y^2 \\ -\dfrac{\partial U_1}{\partial y} - 2\theta \end{Bmatrix} - \begin{Bmatrix} \delta_1 \\ \delta_2 \end{Bmatrix} \tag{32}$$

$$Q_x = -A_{55}U_1 \tag{33}$$

where

$$\psi_{11} = A_{11} - \frac{A_{12}^2}{A_{22}}, \qquad \psi_{22} = D_{66} - \frac{B_{26}^2}{A_{22}}, \qquad \psi_{12} = B_{16} - \frac{A_{12}B_{26}}{A_{22}} \tag{34}$$

$$\delta_1 = N_{xx}^{\mathrm{HT}} - \frac{A_{12}}{A_{22}}N_{yy}^{\mathrm{HT}}, \qquad \delta_2 = M_{xy}^{\mathrm{HT}} - \frac{B_{26}}{A_{22}}N_{yy}^{\mathrm{HT}}$$

The shear stiffness coefficient A_{55} in Eq. (33) does not include any correction factor. A number of shear correction factors have been proposed. Reference 2 presents an approach for improving the shear stiffness coefficient in antisymmetric laminates. The influence of A_{55} on the axial force–twist relationship is shown in Ref. 1 to be small.

Induced Twist due to Curing Stresses

To predict the twist induced by the curing stresses, consider an initially flat laminate subjected to a temperature change ΔT, representing the difference between the cure temperature and the usage temperature, with no change in moisture weight gain percentage. Equations (22), (23), (32), and (33) take the following form:

$$\int_{-b}^{b} N_{xx}^0\,\mathrm{d}y = 0 \tag{35}$$

$$\int_{-b}^{b} \left[N_{xx}^0\theta_0 y^2 - 2M_{xx}^0\right]\mathrm{d}y = 0 \tag{36}$$

$$\begin{Bmatrix} N_{xx}^0 \\ M_{xy}^0 \end{Bmatrix} = \begin{bmatrix} \psi_{11} & \psi_{12} \\ \psi_{12} & \psi_{22} \end{bmatrix} \begin{Bmatrix} \varepsilon_0^0 + \frac{1}{2}(\theta_0 y)^2 \\ -\dfrac{\partial U_1^0}{\partial y} - 2\theta_0 \end{Bmatrix} - \begin{Bmatrix} \bar{\delta}_1 \\ \bar{\delta}_2 \end{Bmatrix} \Delta T \tag{37}$$

$$Q_x^0 = -A_{55}U_1^0 \tag{38}$$

Superscript 0 is associated with the curing stress resultants. The pretwist rate associated with the curing stresses is denoted by θ_0 and

$$\begin{Bmatrix} \bar{\delta}_1 \\ \bar{\delta}_2 \end{Bmatrix} \Delta T = \begin{Bmatrix} \delta_1 \\ \delta_2 \end{Bmatrix} \tag{39}$$

where δ_1 and δ_2 are defined in terms of the thermal forces and moments in Eq. (34). Substitute Eqs. (38) and (37) into Eq. (21) to get

$$\psi_{22}\frac{\partial^2 U_1^0}{\partial y^2} - A_{55}U_1^0 = \psi_{12}\theta_0^2 y \tag{40}$$

Solve Eq. (40) and enforce the free twisting moment conditions at the free edges, Eq. (20), to get the following expression for the warping function:

$$U_1^0 = \frac{\sinh sy}{\psi_{22}s\cosh sb}\left[\psi_{12}\varepsilon_0^0 - 2\psi_{22}\theta_0 + \psi_{12}\left(\frac{\psi_{22}}{A_{55}} + \frac{b^2}{2}\right)\theta_0^2 - \bar{\delta}_2\Delta T\right] - \frac{\psi_{12}}{A_{55}}\theta_0^2 y \tag{41}$$

where

$$s = \sqrt{A_{55}/\psi_{22}} \tag{42}$$

Substitute Eqs. (41), (42), and (37) into Eq. (35) to get, for the axial strain,

$$\varepsilon_0^0 = \frac{1}{k_4}\left(\frac{2\psi_{12}k_1}{\psi_{11}}\theta_0 - \frac{1}{2}b^2k_3\theta_0^2 + \frac{k_5}{\psi_{11}}\Delta T\right) \tag{43}$$

where

$$k_1 = 1 - \frac{\tanh(bs)}{bs}, \qquad k_2 = \frac{2}{3} - k_1\left[1 + \frac{2}{(bs)^2}\right]$$

$$k_3 = \frac{1}{3} - \frac{\psi_{12}^2}{\psi_{11}\psi_{22}}\left(k_2 + \frac{1}{3}\right), \qquad k_4 = \frac{\psi + k_1\psi_{12}^2}{\psi_{11}\psi_{22}} \tag{44}$$

$$k_5 = \bar{\delta}_1 - \frac{\psi_{12}}{\psi_{22}}(1 - k_1)\bar{\delta}_2, \qquad \psi = \psi_{11}\psi_{22} - \psi_{12}^2$$

Substitute Eqs. (37) and (41) into Eq. (36) and substitute for the axial strain ε_0^0 from Eq. (43) to obtain the following temperature–twist relationship:

$$\Delta T(a_3 - a_4\theta_0) = 2\psi\theta_0 + a_1\theta_0^2 + a_2\theta_0^3 \tag{45}$$

where

$$a_1 = \frac{3}{2}b\psi_{11}\psi_{22}\left(k_3 + \frac{k_2k_4}{k_1}\right)$$

$$a_2 = \frac{b^4\psi_{11}^2}{4k_1}\left[k_4\left(k_3 - \frac{2}{15} - \frac{2\psi_{12}^2k_2}{\psi_{11}A_{55}b^2}\right) - k_3^2\right]$$

$$a_3 = \psi_{12}\bar{\delta}_1 - \psi_{11}\bar{\delta}_2, \qquad a_4 = \frac{b^2\psi_{11}}{2k_1}\left(k_3k_5 - \frac{1}{3}k_4k_6\right) \tag{46}$$

$$k_6 = \bar{\delta}_1 - \frac{\psi_{12}}{\psi_{22}}(1 + 3k_2)\bar{\delta}_2$$

The temperature–twist relationship corresponding to the Kirchhoff assumption of no transverse strains can be derived by considering the out-of-plane shear stiffness A_{55} to be very large and consequently the associated shear strain γ_{xz}^0 to vanish. This results in $U_1^0 = 0$ from Eq. (14). By taking the limit as s tends to infinity, equivalent to A_{55} tending to infinity from Eq. (42), coefficients k_i and a_i in Eqs. (44) and (46) reduce to

$$(k_1)_K = (k_4)_K = 1, \qquad (k_3)_K = -(k_2)_K = \frac{1}{3}$$

$$(k_5)_K = (k_6)_K = \bar{\delta}_1, \qquad (a_1)_K = (a_4)_K = 0 \tag{47}$$

$$(a_2)_K = \frac{b^4\psi_{11}^2}{45}, \qquad (a_3)_K = a_3 = \psi_{12}\bar{\delta}_1 - \psi_{11}\bar{\delta}_2$$

where subscript K is the simplified solution based on the Kirchhoff assumption. The associated axial strain–temperature relationship, Eq. (43), reduces to

$$(\varepsilon_0)_{sv} = 2(\psi_{12}/\psi_{11})\theta_0 - \tfrac{1}{6}(\theta_0 b)^2 + (\bar{\delta}_1/\psi_{11})\Delta T \tag{48}$$

and the temperature–twist relationship, Eq. (45), takes the form

$$\Delta T(\psi_{12}\bar{\delta}_1 - \psi_{11}\bar{\delta}_2) = 2\psi\theta_0 + \frac{b^4\psi_{11}^2}{45}\theta_0^3 \tag{49}$$

Neglecting the transverse shear strains allows for an accurate prediction of the extension–twist relationship in the absence of hygrothermal stresses.[1] The accuracy of the simplified temperature–twist relationship is assessed in the Results section by comparing the predictions of Eqs. (45) and (49).

In the next section the axial force–twist relationship for a laminate with initial twist due to the curing stresses and subjected to mechanical loading is derived.

Axial Force–Twist Relationship

Consider a laminate with an initial twist due to curing stresses as given by Eq. (45) or (49) and subjected to mechanical loading. The total axial force N_{xx}^{tot}, twisting moment M_{xy}^{tot}, and shear force Q_x^{tot} per unit middle surface length can be expressed as

$$\begin{Bmatrix} N_{xx}^{\text{tot}} \\ M_{xy}^{\text{tot}} \end{Bmatrix} = \begin{Bmatrix} N_{xx}^0 \\ M_{xy}^0 \end{Bmatrix} + \begin{Bmatrix} N_{xx} \\ M_{xy} \end{Bmatrix} \tag{50}$$

$$Q_x^{\text{tot}} = Q_x^0 + Q_x \tag{51}$$

where N_{xx}^0, M_{xy}^0, and Q_x^0 are the curing stress resultants, which satisfy Eqs. (35–38). The components of the second term on the right-hand side of Eqs. (50) and (51), N_{xx}, M_{xy}, and Q_x, are the mechanical axial force, twisting moment, and shear force obtained from Eqs. (32) and (33) assuming no hygrothermal stress resultants ($\delta_1 = \delta_2 = 0$).

The curing axial force, shear force, and twisting moment satisfy the differential equation (21) and boundary conditions (20), that is,

$$\frac{\partial M_{xy}^0}{\partial y} - Q_x^0 = 0 \tag{52}$$

$$M_{xy}^0\big|_{y=\pm b} = 0 \tag{53}$$

in addition to the boundary conditions (35) and (36).

The total axial force, twisting moment, and shear force satisfy the differential equation (21) and boundary conditions (20), (22), and (23):

$$\frac{\partial M_{xy}^{\text{tot}}}{\partial y} - Q_x^{\text{tot}} = 0 \tag{54}$$

$$M_{xy}^{\text{tot}}\big|_{y=\pm b} = 0 \tag{55}$$

$$\int_{-b}^{b} N_{xx}^{\text{tot}}\,\mathrm{d}y = F \tag{56}$$

$$\int_{-b}^{b}\left[N_{xx}^{\text{tot}}y^2(\theta + \theta_0) - 2M_{xy}^{\text{tot}}\right]\mathrm{d}y = M \tag{57}$$

Because of the small strain assumption, the dimensions of the strip can be assumed to remain within the same bounds for the thermal as well as the mechanical loading. The small warping displacement $-U_1^0 z\hat{\boldsymbol{i}}$, has to be included in Eq. (1) for the position vector in the initial state as mechanical loading is applied. Therefore, U_1 in the strain-displacement relations (14) is actually the difference between the warping functions, $U_1 - U_1^0$. The equilibrium equations and boundary conditions are not affected by this correction. Substitute Eqs. (50–53), (35), and (36) into Eqs. (54–57) to get

$$\frac{\partial M_{xy}}{\partial y} - Q_x = 0 \tag{58}$$

$$M_{xy}|_{y=\pm b} = 0 \tag{59}$$

$$\int_{-b}^{b} N_{xx}\,\mathrm{d}y = F \tag{60}$$

$$\int_{-b}^{b}\left[N_{xx}^0y^2\theta + N_{xx}y^2(\theta + \theta_0) - 2M_{xy}\right]\mathrm{d}y = M \tag{61}$$

Substitute Eqs. (43) and (45) into Eq. (37) to obtain the following expression for the curing axial force per unit length of the middle surface:

$$N_{xx}^0 = \underline{\frac{\psi_{11}}{2}\left(y^2 - \frac{b^2}{3}\right)\theta_0^2} + \psi_{12}\left(\frac{U_1^0(b)}{b} - \frac{\partial U_1^0}{\partial y}\right) \tag{62}$$

The underlined term on the right-hand side of Eq. (62) corresponds to the simplified solution based on the Kirchhoff assumption of no transverse shear strains, whereas the remaining term represents the

contribution of the shear strain and edge effect through the warping function in Eq. (41). This contribution is expressed explicitly in terms of temperature change and initial twist rate as

$$\psi_{12}\left[\frac{U_1^0(b)}{b}-\frac{\partial U_1^0}{\partial y}\right]=\frac{\psi_{12}}{\psi_{11}\psi_{22}k_4}\left(1-k_1-\frac{\cosh sy}{\cosh sb}\right)\times\left[b_3\Delta T-2\psi\theta_0+\psi_{12}\left(\frac{b^2\psi_{11}}{3}+\frac{\psi}{A_{55}}\right)\theta_0^2\right] \tag{63}$$

Substitute from Eq. (63) into Eq. (61) to get

$$\int_{-b}^{b}\left[N_{xx}y^2(\theta+\theta_0)-2M_{xy}\right]\mathrm{d}y=M^* \tag{64}$$

where

$$M^*=M-\underline{\frac{4}{45}\psi_{11}b^5\theta_0^2\theta}+\frac{2\psi_{12}b^3\theta}{3\psi_{11}\psi_{22}k_4}(k_1+3k_2)\times\left[a_3\Delta T-2\psi\theta_0+\psi_{12}\left(\frac{b^2\psi_{11}}{3}+\frac{\psi}{A_{55}}\right)\theta_0^2\right] \tag{65}$$

The underlined term on the right-hand side of Eq. (65) corresponds to the simplified solution. This and the following term represent the contribution of the curing stresses to the total torque.

The axial-force twist relationship for an antisymmetric strip with a pretwist rate θ_0 resulting from the curing stress [Eq. (45) or (49)] and subjected to an axial force F and a torque M^* can now be expressed in a closed form. Substitute for the mechanical axial force N_{xx}, twisting moment M_{xy}, and shear force Q_x from Eqs. (32) and (33) (with $\delta_1=\delta_2=0$) into Eqs. (58), (59), and (64) to get

$$\varepsilon_0(b_4-\theta_0-\theta)=-\frac{1}{2b^3\psi_{11}k_3}T^*+\left(b_1-\frac{4}{3}b_2\theta_0+2b_3\theta_0^2\right)\theta-(b_2-3b_3\theta_0)\theta^2+b_3\theta^3 \tag{66}$$

where

$$b_1=\frac{4\psi_{22}k_1}{b^2\psi_{11}k_3},\qquad b_2=-\frac{3\psi_{12}k_2}{\psi_{11}k_3}$$
$$b_3=\frac{b^3}{2k_3}\left(k_3-\frac{2}{15}-\frac{2\psi_{12}^2k_2}{b^2\psi_{11}A_{55}}\right),\qquad b_4=\frac{2\psi_{12}k_1}{b^2\psi_{11}k_3} \tag{67}$$

Finally, substitute Eq. (32) into Eq. (60) and use Eq. (66) to get

$$F(b_4-\theta_0-\theta)=-\frac{k_4}{b^2k_3}T^*+\left(c_1-\frac{4}{3}c_2\theta_0+2c_3\theta_0^2\right)\theta-(c_2-3c_3\theta_0)\theta^2+c_3\theta^3 \tag{68}$$

where

$$c_1=\frac{8\psi k_1}{b\psi_{11}k_3},\qquad c_2=-6b\psi_{12}\left(k_1+\frac{k_2k_4}{k_3}\right)$$
$$c_3=b^3\psi_{11}\left[\frac{k_4}{k_3}\left(k_3-\frac{2}{15}-\frac{2\psi_{12}^2k_2}{b^2\psi_{11}A_{55}}\right)-k_3\right] \tag{69}$$

and the expressions for k_i are given in Eqs. (44). If the transverse shear strains are neglected, k_i are given in Eqs. (47) and coefficients c_i in Eq. (69) reduce to

$$(c_1)_K=\frac{24\psi}{b\psi_{11}},\qquad (c_2)_K=0$$
$$(c_3)_K=\frac{4b^3\psi_{11}}{45},\qquad (c_4)_K=\frac{6\psi_{12}}{b^2\psi_{11}} \tag{70}$$

where subscript K stands for the Kirchhoff assumption.

Application

Hygrothermally Stable Laminates

In Ref. 1 a set of $[\theta_2/(\theta-90)_4/\theta_2/-\theta_2/(90-\theta)_4/-\theta_2]$ antisymmetric laminates were considered. This stacking sequence has the following properties:

$$A_{11}=A_{22},\qquad B_{16}=-B_{26} \tag{71}$$

and from Eq. (28)

$$N_{xx}^{\mathrm{HT}}=N_{yy}^{\mathrm{HT}},\qquad M_{xy}^{\mathrm{HT}}=0 \tag{72}$$

Substituting Eqs. (71) and (72) into Eq. (34), coefficient a_3 in Eq. (46) or (47) becomes zero. From Eq. (45) or (49) this results in zero pretwist due to the curing cycle. The same result holds if moisture swelling is considered in addition to the temperature change. This class of laminates, proposed by Winckler,[5] will not warp as a result of changes in temperature or moisture and is, therefore, hygrothermally stable. In comparison, angle-ply laminates exhibit higher extension–twist coupling at the expense of hygrothermal stability.

Angle-Ply Laminates

A set of three $[30_4/-30_4]$ laminates was manufactured from T300/954-3 graphite/cyanate material system. The dimensions of the laminate were $298\times25.3\times0.56$ mm. The material properties are listed in Table 1. In-plane Young's moduli E_{11} and E_{22} and Poisson's ratio ν_{12} were obtained from tests of eight-ply unidirectional0- and 90-deg coupons under uniaxial tension loading and the in-plane shear modulus from 45-deg coupons.

The thermal expansion coefficients α_1 and α_2 were first measured using a thermomechanical analyzer. Unidirectional $[0]_8$ and $[90]_8$ coupons with dimensions $25.4\times6.4\times0.56$ mm were cut from $298\times25.4\times0.56$ mm strips and heated. The extension-vs-temperature curves varied with each coupon depending on the location from which it was cut and were not consistently linear. As a result, the measured slopes showed significant scatter.

An alternative method developed in this work accounts for the overall laminate properties. In this method, unidirectional 0- and 90-deg laminates are each bonded to a steel shim stock with a known coefficient of thermal expansion. The bimaterial strip is then exposed to a change in temperature in a cantilevered setup. The coefficients of thermal expansion along the principal material directions are determined from the measured tip displacement. A derivation of the relationship between the coefficients of thermal expansion and tip displacements is provided in the Appendix.

Two $[0]_2$ and $[90]_2$ laminates were each cocured to a 0.44-mm steel shim. The dimensions of each bimaterial strip were $279.4\times22.2\times0.58$ mm. Young's modulus and Poisson's ratio for the steel shim are 190.3 GPa (27.6 Msi) and 0.3, respectively, and the coefficient of thermal expansion is 17.28 $\mathrm{m}\varepsilon/^\circ\mathrm{C}$. Each bimaterial strip was clamped from one end over a distance of 38 mm in a cantilever fixture and placed in an industrial oven with a glass door. The tip deflection was monitored as the strip was heated. Readings were taken within a temperature range from 100°F (37.8°C) to 225°F (107.2°C) at 25°F (13.9°C) intervals. Two tests were performed using each strip, and the data showed consistent trends and were repeatable. The thermal expansion coefficients in Table 1 are the average values obtained from all four tests for each principal material direction.

After curing, the measured end twists were 63.2, 62.2, and 64.9 deg with an average value of 63.4 deg for a temperature variation $\Delta T=-138^\circ\mathrm{C}$, corresponding to the cooling process from cure temperature to room temperature. The predictions of Eqs. (45)

Table 1 Properties of T300/954-3 graphite/cyanate material system

$E_{11}=135.6$ GPa (19.7 Msi)
$E_{22}=E_{33}=9.9$ GPa (1.4 Msi)
$G_{12}=G_{13}=4.2$ GPa (0.6 Msi)
$G_{23}=2.5$ GPa (0.36 Msi)
$\nu_{12}=\nu_{13}=0.3$
$\nu_{23}=0.5$
$\alpha_1=4.34\ \mathrm{m}\varepsilon/^\circ\mathrm{C}$ (2.41 $\mathrm{m}\varepsilon/^\circ\mathrm{F}$)
$\alpha_2=37.0\ \mathrm{m}\varepsilon/^\circ\mathrm{C}$ (20.6 $\mathrm{m}\varepsilon/^\circ\mathrm{F}$)
Ply thickness = 0.073 mm (0.00287 in.)

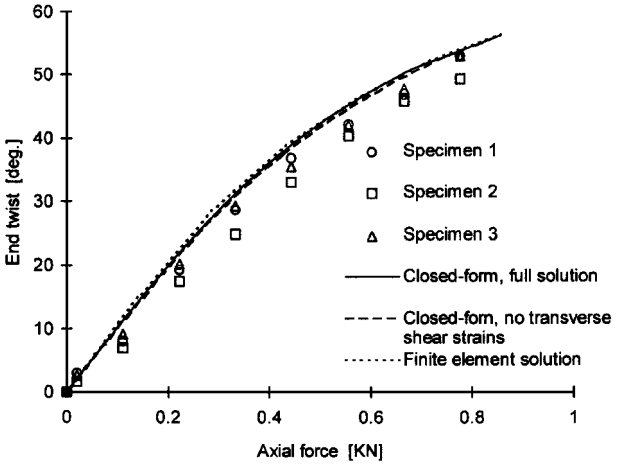

Fig. 2 Comparison of analytical and finite element solutions with test data.

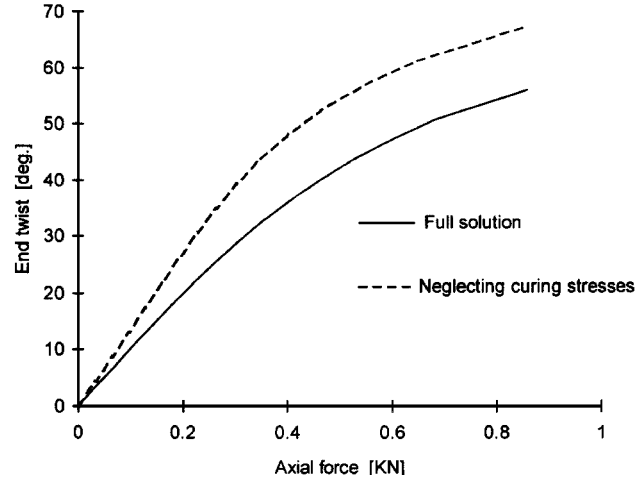

Fig. 3 Influence of curing stresses on the axial force–twist behavior.

and (49) are 64.4 and 64.0 deg, respectively, corresponding to 1.6 and 1.0% differences relative to the average test data. The prediction of the linear theory, corresponding to the first term on the right-hand side of Eq. (49), is 101.5 deg, resulting in a 60.1% difference relative to the average test data.

A nonlinear finite element analysis was performed with thermal and axial loading using the ABAQUS code. The element used was an S4R quadrilateral shell element. The total number of elements was 200, corresponding to 691 nodes and 4146 degrees of freedom. A temperature decrement of 138°C was first applied in the analysis, and the resulting twist was 65.8 deg. This corresponds to a 3.9% difference relative to the average test data. Axial load was then incremented, and the associated end rotation was computed at specific intervals. Figure 2 shows the end twist vs applied axial load as predicted by the finite element analysis and the closed-form solution, Eqs. (68) and (65) with zero applied torque M. The prediction of the simplified solution labeled "closed-form, no transverse shear strains" in Fig. 2 and corresponding to the underlined term only in Eq. (65) is indistinguishable from the full solution. Also appearing in Fig. 2 are the test data from the three laminates.

The testing was performed in an Instron machine using the patented rotational displacement apparatus[6] developed in Ref. 7. This apparatus uses air as a bearing medium to allow for free end twist as axial load is applied. The apparatus fits into a universal testing machine with one end of the laminate clamped to its shaft and with the other to the testing machine. A differential pressure is applied to the apparatus, and the resultant load is measured by the testing machine load cell. The angle of twist was measured over a 25.4-cm (10-in.) gauge length and was read by a digital display.

One challenging feature for testing these highly pretwisted laminates is their stability. Equation (66) indicates that their effective torsional rigidity depends on the axial strain. Therefore, the pretwisted strips are prone to torsion–bending instability when axial load is applied. This is more significant in angle-ply laminates such as $[30/-30]$ due to their relatively low axial stiffness. To eliminate any compressive preload, the air bearing apparatus was placed at the lower end of the laminate. The repeatability of the data from the three specimens illustrates the ability of the air bearing apparatus to accommodate such highly pretwisted laminates. The correlation coefficients for the finite element, closed-form full solution, and Saint Vénant-type solution in Fig. 2 are 0.960, 0.975, and 0.988, respectively.

Finally an assessment of the influence of the curing stresses on the extension–twist coupling in the $[30_4/-30_4]$ angle-ply laminates is performed. The contribution of the curing stresses to the total torque in the axial force–twist relationship is represented by the difference between M^* and M in Eq. (65). Because the laminate is subjected to axial force only and is free to twist, the torque $M = 0$. Figure 3 shows a comparison between the predictions of the full solution in Eq. (68) with M^* given in Eq. (65) and the solution neglecting curing stresses, i.e., $M^* = M = 0$. Neglecting the contribution of the curing stresses could lead to a percentage error as high as 20%.

Conclusion

A finite displacement model for the prediction of extension–twist coupling in pretwisted laminated composite strips in the presence of hygrothermal stresses is developed. A closed-form expression for the initial twist associated with the curing stresses in antisymmetric laminates is obtained, and the contribution of the transverse shear strains is isolated. A closed-form solution for the axial-force twist relationship is derived. An assessment of the accuracy of the developed solution is provided through comparison of predictions with a nonlinear finite element solution and test data from antisymmetric angle-ply laminates made of graphite/cyanate material. The predictions of the developed solution are in good agreement with the test data and finite element simulation. It is found that neglecting transverse shear strains has a negligible influence on the results. The influence of the curing stresses on the axial force–twist behavior is significant.

Appendix: Determination of the Thermal Expansion Coefficients

Consider a thin bimaterial strip made out of a unidirectional composite laminate of thickness h_1 and plane stress reduced stiffness coefficients $Q_{ij}^{(1)}$, bonded to an isotropic layer of thickness h_2, with Young's modulus E and Poisson's ratio ν. The plane stress reduced stiffness coefficients of the isotropic layer will be denoted by $Q_{ij}^{(2)}$. The strip has a length L and total thickness h and is supported in a cantilevered configuration and subjected to a temperature change ΔT. A straight line element perpendicular to the middle surface of the strip is assumed to remain straight, normal to the deformed middle surface, and inextensible. The curvatures associated with the deformed middle surface are assumed constant. The strains and curvatures are assumed small, that is,

$$\varepsilon^0_{\max}, \qquad h\kappa_{\max} \ll 1 \tag{A1}$$

where $\varepsilon^0_{\max}$ and $\kappa_{\max}$ are the maximum values of the middle surface strains and curvatures.

The constitutive relationships for the strip, Eq. (24), simplify to

$$\begin{Bmatrix} N_{xx} \\ N_{yy} \\ M_{xx} \\ M_{yy} \end{Bmatrix}^{\mathrm{HT}} = \begin{bmatrix} A_{11} & A_{12} & B_{11} & B_{12} \\ A_{12} & A_{22} & B_{12} & B_{22} \\ B_{11} & B_{12} & D_{11} & D_{12} \\ B_{12} & B_{22} & D_{12} & D_{22} \end{bmatrix} \begin{Bmatrix} \varepsilon^0_{xx} \\ \varepsilon^0_{yy} \\ -\kappa_{xx} \\ -\kappa_{yy} \end{Bmatrix} \tag{A2}$$

where

$$\begin{gathered} A_{ij} = h_1 Q_{ij}^{(1)} + h_2 Q_{ij}^{(2)}, \qquad B_{ij} = (h_1 h_2/2)\left[Q_{ij}^{(1)} - Q_{ij}^{(2)}\right] \\ D_{ij} = \tfrac{1}{12}\left[h_1\left(h_1^2 + 3h_2^2\right)Q_{ij}^{(1)} + h_2\left(h_2^2 + 3h_1^2\right)Q_{ij}^{(2)}\right] \\ N_{ii}^{\mathrm{HT}} = \left[h_1\alpha_j^{(1)}Q_{ij}^{(1)} + h_2\alpha_j^{(2)}Q_{ij}^{(2)}\right]\Delta T \\ M_{ii}^{\mathrm{HT}} = (h_1 h_2/2)\left[\alpha_j^{(1)}Q_{ij}^{(1)} - \alpha_j^{(2)}Q_{ij}^{(2)}\right]\Delta T \qquad (i = x, y) \end{gathered} \tag{A3}$$

Summation over index j is implied in the expressions for N_{ii} and M_{ii}. A reference rectangular Cartesian coordinate system x, y, z is adopted for convenience with y–z coinciding with the strip cross section. The x axis is taken along the strip central axis. The strip is fixed at $x = 0$ and free at $x = L$. The transverse deflection at the free endpoint $x = L$, $y = 0$ is expressed as

$$w_L = \frac{1}{\kappa_{xx}}[1 - \cos(\kappa_{xx} L)] \approx \frac{\kappa_{xx} L^2}{2} \tag{A4}$$

where the transverse displacement is approximated by the small displacement relationship by considering $\kappa_{xx} L^2/12$ negligible compared to 1. Substitute from Eq. (A3) into (A2) and solve for κ_{xx} to get a linear function in terms of the coefficients of thermal expansion:

$$\kappa_{xx} = \alpha c_0^{(1)} + \alpha_1 c_1^{(1)} + \alpha_2 c_2^{(1)} \tag{A5}$$

where α is the linear coefficient of thermal expansion of the isotropic layer and α_1 and α_2 are the linear coefficients of thermal expansion along the principal material directions. Coefficients $c_i^{(1)}$ are defined in terms of the stiffness coefficients of the bimaterial strip:

$$c_0^{(1)} = -h_2 \frac{E}{(1-v)} \left[b_{11} + b_{12} - \frac{h_1}{2}(d_{11} + d_{12}) \right] \Delta T$$

$$c_1^{(1)} = -h_1 \left[Q_{11}^{(1)} b_{11} + Q_{12}^{(1)} b_{12} + \frac{h_2}{2}\left(Q_{11}^{(1)} d_{11} + Q_{12}^{(1)} d_{12} \right) \right] \Delta T \tag{A6}$$

$$c_2^{(1)} = -h_1 \left[Q_{12}^{(1)} b_{11} + Q_{22}^{(1)} b_{12} + \frac{h_2}{2}\left(Q_{12}^{(1)} d_{11} + Q_{22}^{(1)} d_{12} \right) \right] \Delta T$$

where

$$\begin{bmatrix} a_{11} & a_{12} & b_{11} & b_{12} \\ a_{12} & a_{22} & b_{12} & b_{22} \\ b_{11} & b_{12} & d_{11} & d_{12} \\ b_{12} & b_{22} & d_{12} & d_{22} \end{bmatrix} = \begin{bmatrix} A_{11} & A_{12} & B_{11} & B_{12} \\ A_{12} & A_{22} & B_{12} & B_{22} \\ B_{11} & B_{12} & D_{11} & D_{12} \\ B_{12} & B_{22} & D_{12} & D_{22} \end{bmatrix}^{-1} \tag{A7}$$

By measuring the transverse displacement w_L from two bimaterial strips, one with a [0] unidirectional laminate and the other with a [90] laminate, each cocured to a steel shim, the coefficients of thermal expansion α_1 and α_2 could be determined. Denote the curvature associated with the [0] strip by $\kappa_{xx}^{(1)}$. Its relationship to the coefficients of thermal expansion is given in Eqs. (A5) and (A6). The curvature associated with the [90] strip is given by

$$\kappa_{xx}^{(2)} = \alpha c_0^{(2)} + \alpha_1 c_1^{(2)} + \alpha_2 c_2^{(2)} \tag{A8}$$

where

$$c_0^{(1)} = -h_2 \frac{E}{(1-v)} \left[b_{12} + b_{22} - \frac{h_1}{2}(d_{12} + d_{22}) \right] \Delta T$$

$$c_1^{(1)} = -h_1 \left[Q_{11}^{(1)} b_{12} + Q_{12}^{(1)} b_{22} + \frac{h_2}{2}\left(Q_{11}^{(1)} d_{12} + Q_{12}^{(1)} d_{22} \right) \right] \Delta T \tag{A9}$$

$$c_2^{(1)} = -h_1 \left[Q_{12}^{(1)} b_{12} + Q_{22}^{(1)} b_{22} + \frac{h_2}{2}\left(Q_{12}^{(1)} d_{12} + Q_{22}^{(1)} d_{22} \right) \right] \Delta T$$

Solve Eqs. (A5) and (A8) to get

$$\begin{Bmatrix} \alpha_1 \\ \alpha_2 \end{Bmatrix} = \frac{1}{\left(c_1^{(1)} c_2^{(2)} - c_1^{(2)} c_2^{(1)} \right)} \begin{bmatrix} c_2^{(2)} & -c_2^{(1)} \\ -c_1^{(2)} & c_1^{(1)} \end{bmatrix} \begin{Bmatrix} \kappa_{xx}^{(1)} - \alpha c_0^{(1)} \\ \kappa_{xx}^{(2)} - \alpha c_0^{(2)} \end{Bmatrix} \tag{A10}$$

A simplified one-dimensional model could be derived by assuming the cross section of the strip to be rigid. This is achieved by neglecting Poisson's contribution to the stiffness coefficients:

Table A1 Comparison of thermal coefficients from one-dimensional and two-dimensional analyses

Equation	α_1	α_2
Two dimensional, Eq. (A10)	$4.34 \times 10^{-6}/^{\circ}\mathrm{C}$	$37.0 \times 10^{-6}/^{\circ}\mathrm{C}$
One dimensional, Eq. (A13)	$4.35 \times 10^{-6}/^{\circ}\mathrm{C}$	$36.2 \times 10^{-6}/^{\circ}\mathrm{C}$

$$Q_{12}^{(1)} = Q_{12}^{(2)} = A_{12} = B_{12} = D_{12} = 0 \tag{A11}$$

Consequently coefficients $c_2^{(1)}$ and $c_1^{(2)}$ in Eqs. (A5) and (A8) vanish. The remaining coefficients simplify to

$$c_0^{(i)} = -c_i^{(i)} = 6(h_1 + h_2)\Delta T \Bigg/ \left[\left(\frac{E_{ii} h_1}{E h_2} + 4 \right) h_1^2 + \left(\frac{E h_2}{E_{ii} h_1} + 4 \right) h_2^2 + 6 h_1 h_2 \right] \qquad (i = 1, 2) \tag{A12}$$

In this case, the two equations in (A10) decouple and the [0] strip provides α_1, whereas the [90] strip provides α_2. Substitute from Eq. (A12) into Eq. (A10) with $c_2^{(1)} = c_1^{(2)} = 0$ to get the following expressions for the thermal expansion coefficients in terms of the transverse displacement:

$$\alpha_i = \alpha - \frac{w_L}{3L^2} \left\{ \left[\left(\frac{E_{ii} h_1}{E h_2} + 4 \right) h_1^2 + \left(\frac{E h_2}{E_{ii} h_1} + 4 \right) h_2^2 + 6 h_1 h_2 \right] \Bigg/ (h_1 + h_2)\Delta T \right\} \qquad (i = 1, 2) \tag{A13}$$

An assessment of the two-dimensional and one-dimensional analyses in Eqs. (A10) and (A13) is provided by comparing their predictions for the [0] and [90] graphite/cyanate-steel strips. The average curvatures obtained from the test data for $\Delta T = 55.6^{\circ}\mathrm{C}$ (100°F) are

$$\kappa_{xx} = 0.0948/\,\mathrm{m}, \qquad \kappa_{yy} = -0.456/\,\mathrm{m} \tag{A14}$$

The associated coefficients of thermal expansion as predicted by Eqs. (A10) and (A13) are given in Table A1.

Acknowledgment

This work is sponsored by the National Rotorcraft Technology Center under Grant NCC2-945. This support is gratefully acknowledged.

References

[1] Armanios, E. A., Makeev, A., and Hooke, D. A., "Finite-Displacement Analysis of Laminated Composite Strips with Extension-Twist Coupling," *Journal of Aerospace Engineering*, Vol. 9, No. 3, 1996, pp. 80–91.

[2] Makeev, A., and Armanios, E., "On a Higher Order Analysis of Laminated Composite Strips with Extension–Twist Coupling," *International Journal of Solids and Structures* (to be published).

[3] Sokolnikoff, I. S., *Tensor Analysis*, Wiley, New York, 1951.

[4] Vinson, J. R., and Sierakowski, R. L., *The Behavior of Structures Composed of Composite Materials*, Martinus–Nijhoff, Dordrecht, The Netherlands, 1986.

[5] Winckler, S. I., "Hygrothermally Curvature Stable Laminates with Tension-Torsion Coupling," *Journal of the American Helicopter Society*, Vol. 31, No. 7, 1985, pp. 56–58.

[6] Hooke, D. A., and Armanios, E. A., "Rotational Displacement Apparatus with Ultra-Low Torque and High Thrust Load Capability," U.S. Patent 5,661,247, Aug. 1997.

[7] Hooke, D. A., and Armanios, E. A., "Design and Evaluation of Three Methods for Testing Extension-Twist-Coupled Laminates," *Composite Materials: Testing and Design*, ASTM STP 1274, edited by C. R. Saff and R. B. Deo, Vol. 12, American Society for Testing and Materials, New York, 1996, pp. 340–357.

A. M. Waas
Associate Editor